Russian Journal of Earth Sciences

Surface Transport of Technical Waters from Fukushima NPP to the South Kuril Fishing Zone

M. V. Budyansky[1,2*], T. V. Belonenko[1], M. A. Lebedeva[1,2], and A. A. Udalov[2]

[1] St. Petersburg State University, St. Petersburg, Russia
[2] Il'ichev Pacific Oceanological Institute FEB RAS, Vladivostok, Russia
* **Correspondence to:** Tatyana Belonenko, btvlisab@yandex.ru

Abstract: This study explores the potential for the penetration of technical waters from the Fukushima nuclear power plant (Fukushima NPP) into the fishing areas of Russia. Using a Lagrangian approach, which examines the advection of a large number of passive markers simulating waters released from the Fukushima NPP, the typical transport pathways to the South Kuril Islands are investigated, and an estimate of the time of such transport is provided. Calculations are conducted using satellite-derived and modelled velocity fields for the test year from August 24, 2022, to August 24, 2023. This study focuses on the advection of Lagrangian markers and highlights the potential for the rapid arrival of them from the Fukushima NPP into the southern Kuril region. This article emphasizes the importance of considering the seasonal variability in Kuroshio meandering and the impact of local mesoscale vortex advection related to the propagation of Lagrangian markers from the Fukushima NPP.

Keywords: Fukushima nuclear power plant, Lagrangian markers, South Kuril region, simulation, simulated particles, advection, vortex.

Citation: Budyansky, M. V., T. V. Belonenko, M. A. Lebedeva, and A. A. Udalov (2024), Surface Transport of Technical Waters from Fukushima NPP to the South Kuril Fishing Zone, *Russian Journal of Earth Sciences*, 24, ES4002, EDN: VQKJUM, https://doi.org/10.2205/2024es000934

1. Introduction

The powerful earthquake and subsequent catastrophic tsunami that struck the north-eastern coast of Honshu Island, Japan, on March 11, 2011, caused a technological disaster at the Fukushima NPP, alongside significant human casualties and extensive destruction of coastal settlements. This incident led to widespread radioactive contamination of the atmosphere and Pacific waters east of Japan. Numerous residents in the Sakhalin region, Russia, expressed apprehension regarding the potential transport of radioactive waters to the shores of the southern Kuril Islands and the subsequent radioactive contamination of fish and other seafood products entering the market. These concerns have not completely disappeared even today.

In 2011, a substantial amount of debris, including cars, refrigerators, house fragments, and other waste, was swept from the Japanese coast. These materials coalesced into dense masses that ultimately reached the shores of the USA, following the primary path of the Kuroshio Current and the North Pacific Ocean Current [*NOAA*, 2013]. However, there was a tangible risk concerning potential contamination of waters in the northwestern region of the Pacific Ocean. These areas are rich in fish and squid [*Buslov*, 2013]. The economic importance of the northwestern part of the Pacific Ocean is mainly associated with its substantial bioproductivity, a characteristic significantly influenced by oceanographic conditions.

Currently, a significant amount of water that is used to cool reactors has accumulated at operational stations. Following the incident at the Fukushima NPP in March 2011, seawater remains necessary for cooling the reactor cores. The "contaminated" water, containing radionuclides, has been gathered in tanks and subjected to treatment at the Fukushima NPP site. Despite objections from neighbouring countries, primarily Russia

Research Article

Received: 27 May 2024
Accepted: 29 August 2024
Published: 14 October 2024

and China, the International Atomic Energy Agency (IAEA) gave consent for the discharge of "contaminated" water. In 2021, the Japanese government made the decision to progressively release treated water into the Pacific Ocean, commencing on August 24, 2023, with a planned duration extending over the next three decades.

In Figure 1, the study area is depicted along with a generalized schematic representation of the main currents. The oceanographic conditions in the region are characterized by significant heterogeneity and spatiotemporal variability. From the Pacific side, the Kuril Islands are bathed by the Oyashio Current, an extension of the East Kamchatka Current. The Oyashio Current intensifies in the vicinity of the Bussol Strait due to the inflow of waters from the Sea of Okhotsk. North of the Bussol Strait, the Oyashio Current tends to weaken, but to the south, after the influx of Okhotsk Sea waters occurs, its flow strengthens, and the discharge increases threefold [*Belonenko et al.*, 1997; *Kawai*, 2013]. The main branches of the Oyashio Current, the first and the second, are the most stable. The first follows along the shelf and slope depths toward Hokkaido, while the second moves south or southwest of Iturup. In addition to the cold waters from the Sea of Okhotsk flowing through the Ekaterina and Friz straits, the warm Soya Current also enters the southern Kuril region of the Pacific Ocean. Complex vortex formations in this region are generated and intensified by the opposing movement of the northeast branch of the Kuroshio. Its main current wedges between the first and second branches of the Oyashio [*Itoh and Yasuda*, 2010].

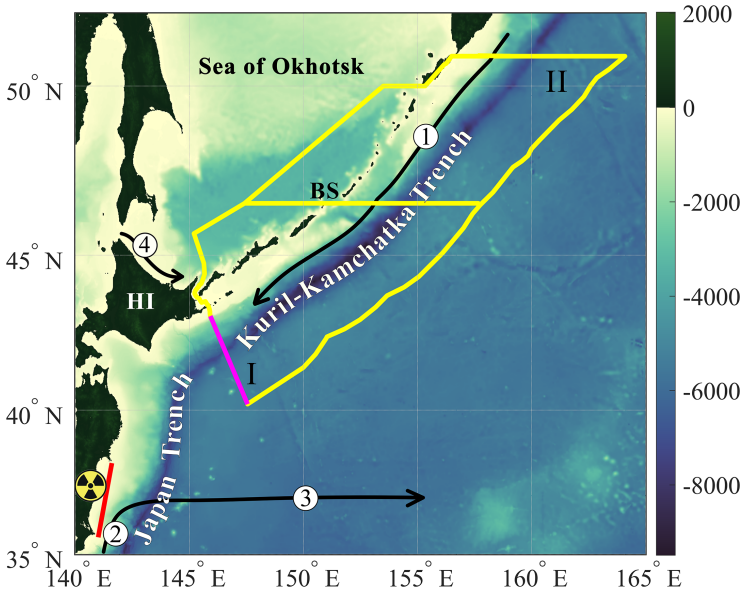

Figure 1. The study area. The location of the Fukushima NPP (coordinates 37°25'12.0" N, 141°2'58.0" E) is indicated by the radiation hazard symbol ☢. The yellow line represents the boundaries of the South Kuril Fishing Zone (SKFZ) – I and North Kuril Fishing Zone (NKFZ) – II. The pink segment denotes the southwest border of the SKFZ. The red segment (35.6°N, 141°E–38.3°N, 141.6°E) is located near the Fukushima NPP (trajectories of simulated particles start here). The bottom topography is shown in colour shading. The boundaries of the SKFZ and NKFZ were determined according to the government documents of the Russian Federation. 1 – the Oyashio Current, an extension of the East Kamchatka Current, 2 – the Kuroshio Current, 3 – the Kuroshio Extension, and 4 – Soya Current; HI – Hokkaido Island and BS – Bussol Strait.

The area under investigation is commonly referred to as the Kuroshio-Oyashio confluence zone or a subarctic frontal area [*Belonenko et al.*, 1997; *Kawai*, 2013]. Here, the Kuroshio Extension lengthens the Kuroshio Current, which changes its course to the east at approximately 35°. This results in a strong, meandering jet forming a boundary between warm subtropical and cold subarctic waters. This region undergoes an exceptionally robust exchange of heat between the atmosphere and the ocean, exhibiting the highest level of

eddy kinetic energy. The Kuroshio-Oyashio confluence zone is rich in diverse mesoscale eddies that play a crucial role in facilitating the transfer of heat, salt, nutrients, carbon, pollutants, and other tracers across the ocean.

At the southern Kuril Islands, powerful anticyclonic eddies form as a result of the detachment of warm tongues and meanders of the Kuroshio. These eddies are long-lived, with lifespans ranging from 2 to 3 months to several years [*Travkin et al.*, 2022; *Udalov et al.*, 2023]. Interestingly, upon entering the southern Kuril region, mesoscale eddies continue to move northeastward along the Kuril Trench. They pass over deep-sea trenches not close to the coast, and most often, they disintegrate near the islands of Urup and Iturup [*Udalov et al.*, 2023]. The described dynamics and variability of oceanographic conditions in the waters near the Kuril Islands are reflected in the abundance and composition of the biota in this region. Extending from the Kamchatka Peninsula to Hokkaido Island, this area plays a crucial role in Russia's fishing industry, serving as a hub for the industrial exploitation of aquatic resources [*Buslov*, 2013; *Shuntov*, 2022].

The basis of the fishery in the region is fish. On average, over this period, it amounted to almost 80%. In addition to fish, there was a significant harvest of molluscs. These organisms are harvested using vessels of various types [*Buslov*, 2013]. This region is a crucial Russian area for the fishing of fish and squid, holding immense significance for ensuring Russia's food security. How the discharge of polluted waters from the Fukushima NPP will affect fish and squid is a matter of research for future years.

The issues of radioactive contamination are actively studied from the perspective of continuous dosimetry and numerical modelling of radioactive contamination involving various radionuclides [*Budyansky et al.*, 2015; *Prants*, 2014; *Prants et al.*, 2017a]. However, this particular work is dedicated to assessing the time and pathways of the potential spread of contamination into fishing areas, in which we assess the time and pathways of the potential spread of contamination into fishing areas [*Maderich et al.*, 2024]. *Smith et al.* [2023] declare that fears of radiation are likely to damage the livelihoods of fishing communities lying in the path of Fukushima NPP waters, which is still recovering from fishing bans and reputational damage caused by the 2011 accident. Although radiation protection science unequivocally asserts today that the planned release of Fukushima wastewater poses no substantial threat to Pacific Ocean organisms or consumers of seafood impacted by Fukushima PP discharge governments and researchers worldwide are expected to closely monitor radioactivity in the Pacific Ocean during the release [*IAEA*, 2018, 2023].

We focus only on the advection of marker tracers from the Fukushima NPP into the areas of Russian coastal waters in this paper. We do not provide a quantitative assessment concentration assessment of the more than 62 radionuclides discharged into the water, which the Advanced Liquid Processing System cannot remove [*TEPCO*, 2023]. We study here only the pathways and mechanisms of Lagrangian marker advection which can reach the southern Kuril region from the Fukushima NPP. In this study, we call the Lagrangian markers which advection start from the Fukushima NPP the simulated particles. This analysis is extremely important because the release of "contaminated" radioactive water from Fukushima NPP is planned to take place in the future over an extended period. It is worth noting that ocean circulation and advection of water in this small area have never been studied in detail before.

We examine one year from August 24, 2022, to August 24, 2023. In other words, we are analysing the scenario of what would have happened with the spread of radioactive waters in the region if the release of "contaminated" water had occurred on August 24, 2022. We also consider the dependence of marker numbers on seasons and reveal the months when the number of these markers in the South Kuril region is the largest. The study area is in the South Kuril Fishing Zone (SKFZ) where commercial fishing of fish and squid is conducted (Figure 1).

2. Methods

Lagrangian modelling is employed to study the transport properties of fluid elements [*Budyansky et al.*, 2015; *Prants*, 2014; *Prants et al.*, 2017a,b,c]. Lagrangian modelling enables the study of the paths and durations of dispersion of water parcels with a high degree of accuracy. For this purpose, we use a marker tracking method. This method involves calculating a large number of trajectories for passive tracers simulating contamination in the SKFZ. The simulation of water circulation in oceanic basins is effectively performed using Lagrangian methods, which provide a detailed account of transport and mixing within a specific area by calculating the trajectories of numerous artificial passive particles. In turbulent or chaotic flows, visualizing trajectories of particles advected by satellite-derived or numerical-model velocity fields results in a complex web of intertwined paths that can be challenging to interpret [*Prants et al.*, 2017c].

To utilize the Lagrangian approach, a dense mesh of artificial particles is numerically advected backward and forward in time from a fixed date.

By analysing the simulation results in reverse time, researchers can determine the origins of fluid particles passing through specific points. This approach is particularly valuable for studying circulation in basins with only a few incoming water masses, such as the study area. The trajectories of Lagrangian particles are computed by solving the advection equations

$$\frac{\mathrm{d}\lambda}{\mathrm{d}t} = u(\lambda, \varphi, t), \quad \frac{\mathrm{d}\varphi}{\mathrm{d}t} = v(\lambda, \varphi, t), \tag{1}$$

where u and v are the angular zonal and meridional components of the AVISO or GLORYS12V1 (NEMO) velocity field, respectively, and φ and λ are the latitude and longitude, respectively.

Angular velocities are employed due to their simplicity in equations when dealing with the Earth's spherical geometry. To ensure precise numerical results, bicubic spatial interpolation and temporal smoothing using third-order Lagrangian polynomials are applied. The Lagrangian trajectories are calculated by integrating equations (1) utilizing the fourth-order Runge-Kutta scheme with a fixed time step of 0.001 days. This meticulous numerical approach ensures accurate simulations and reliable results.

In the present study, stationary points in the velocity field on a given date are marked on geographical maps with triangles and crosses. Elliptic stationary points, shown as triangles and located at the centers of vortices, are points around which the movement is stable and circular. Hyperbolic stationary points, shown as crosses, are situated between the vortices and are unstable, with two directions along which the waters converge to such a point, and two others along which they diverge [*Budyansky et al.*, 2015; *Prants*, 2014; *Prants et al.*, 2017a,b,c].

3. Data

To construct Eulerian flow maps, we utilize two sources of information: geostrophic velocities based on AVISO satellite altimetry data with a spatial resolution of 1/4° and current velocities on the 0.5 m depth level obtained from the global high-resolution ocean reanalysis GLORYS12V1 (Global Ocean Physics Reanalysis) with a spatial resolution of 1/12°, created using NEMO (Nucleus for European Modelling of the Ocean). Both products are available on the Copernicus Marine Environment Monitoring Service portal (CMEMS) (https://data.marine.copernicus.eu/product/GLOBAL_ANALYSISFORECAST_PHY_001_024/description). The study covers one period from August 24, 2022, to August 24, 2023. The Lagrangian modelling algorithms are configured for calculations based on data from one year ago. Essentially, we use a two-year dataset from AVISO and GLORYS12V1 (NEMO) spanning from August 24, 2021, to August 24, 2023.

a. Geostrophic currents from the merged altimeter data

The geostrophic velocities from AVISO are the result of merged measurements from all altimetric missions – Jason-3, Sentinel-3A, HY-2A, Saral/AltiKa, CryoSat-2, Jason-2,

Jason-1, T/P, ENVISAT, GFO, and ERS1/2 – covering the period from 1993 to the present. The data were merged via the optimal interpolation method [*CMEMS*, 2020]. The spatial averaging of the data was performed at a resolution of 1/4° latitude and longitude, with a temporal resolution of 1 day.

The idea of using the AVISO velocity field for the advection of passive markers simulating radioactive contamination is not new and has been used by the authors before. It is a region of strongly seasonal water mass formation for mode waters of varying flavors and evolution [*Dong et al.*, 2017; *Kawakami et al.*, 2015; *Oka and Qiu*, 2011; *Oka et al.*, 2011; *Qiu et al.*, 2006; *Suga and Hanawa*, 1995; *Zhang et al.*, 2021]. The 2012 research expedition conducted by the V. I. Il'ichev Pacific Oceanological Institute of the Far Eastern Branch of the Russian Academy of Sciences revealed that, despite the subduction of radioactive contamination to depths of 100–500 meters within anticyclones, concentrations of simulated particles, as determined by AVISO, exhibited a strong correlation with field dosimetry data [*Budyansky et al.*, 2015].

b. Currents from the GLORYS12V1 (NEMO) reanalysis

The GLORYS12V1 (NEMO) product is based on a global real-time forecasting system. The model relies on the NEMO model with forcing from the ECMWF ERA-Interim dataset. The GLORYS12V1 (NEMO) product assimilates in situ and satellite data from missions such as Topex/Poseidon, Jason-1, 2, MODIS Terra/Aqua, and AVHRR NOAA, as well as from drifting buoys such as Argo and drifters, other natural observations, and oceanographic surveys. Observations are assimilated into the NEMO model using a low-order Kalman filter. GLORYS12V1 (NEMO) accurately captures intricate surface dynamics at a small scale and shows robust agreement with independent data not included in the assimilation process. GLORYS12V1 (NEMO) offers a dependable representation of the physical ocean state, making it valuable for studying many ocean exploration tasks and enabling applications such as seasonal forecasts. Moreover, its high-quality data make it a valuable resource for regional purposes and provide essential physical parameters for areas such as marine biogeochemistry [*Lellouche et al.*, 2021]. We used geostrophic velocities on a 0.5 m depth level. The spatial average of the data was taken at 1/12° latitude and longitude, with a temporal resolution of 1 day.

4. Results

4.1. Ocean Circulation in the Research Area Using AVISO and GLORYS12V1 (NEMO) Data

The research area to the east of Japan is bounded to the south and north by the meandering currents of the strong warm Kuroshio current and the cold Oyashio current. These currents coincide with their respective hydrological fronts. The segment of the Kuroshio system from the island of Honshu to the Imperial Mountains is called the Kuroshio Extension. At approximately 42°–43°N latitude, the Oyashio current turns eastwards (this is known as the Second Branch of the Oyashio). The region where the Kuroshio and Oyashio interact is one of the most dynamically active areas in the world ocean and exhibits variability in oceanographic fields over a wide range of spatial and temporal scales [*Belonenko et al.*, 2009]. Observations indicate that at certain intervals, the Kuroshio and Oyashio currents split into individual branches, indicating the bifurcation of the currents.

The strength (transport) of the Kuroshio varies along its path and seasonally, with a speed reaching 2.5 m/s [*Qu et al.*, 2001]. The velocities in the Oyashio Current are significantly lower than those in the other regions, and in February, they reach 0.5–1.0 m/s. However, in summer, the Oyashio current significantly weakens, with speeds not exceeding 0.25–0.35 m/s [*Belonenko et al.*, 1997]. This process facilitates the penetration of water from the south, mixing water of different origins, and detachment of filaments from eddies, ultimately leading to the entry of potentially "contaminated" waters into the North Pacific Ocean. Figure 2 shows the mean currents averaged for September 2022 and April 2023. The calculations were performed using altimetry data and GLORYS12V1 (NEMO) data.

The meandering Kuroshio current, characterized by high velocities, is highlighted in dark colour. The transport of the Kuroshio near the coast of Japan reaches 65 Sv (1 Sv = 10^6 m^3/s), but this transport exhibits pronounced seasonal variability [*Sekine and Kutsuwada*, 1994]. Figure 2 clearly shows that the spatial position of the Kuroshio current changes. In April, the current forms a meander close to Hokkaido Island, adjacent to the part of the coast where the Fukushima NPP is located. In September, this meander shifts eastwards by approximately 200 km, creating a loop that eventually detaches from the main current, forming the so-called Kuroshio Ring [*Tomosada*, 1986]. The seasonal variability in the Kuroshio current can impact the transport of potentially "contaminated" waters toward the Kuril shores and the Russian fish and squid harvesting area. Figure 2 displays the northern branch of the Kuroshio Extension, recognized as the North Pacific Current. This current originated from the interaction between the Kuroshio current, which shifts northward along the coast of Japan, and the Oyashio current, a cold subarctic current that flows southward and circulates counterclockwise along the western region of the northern Pacific Ocean [*Venti and Billups*, 2013]. The speed of the North Pacific Current decreases from west to east, ranging from approximately 0.5 to 0.1 m/s, with transport of 15–35 Sv.

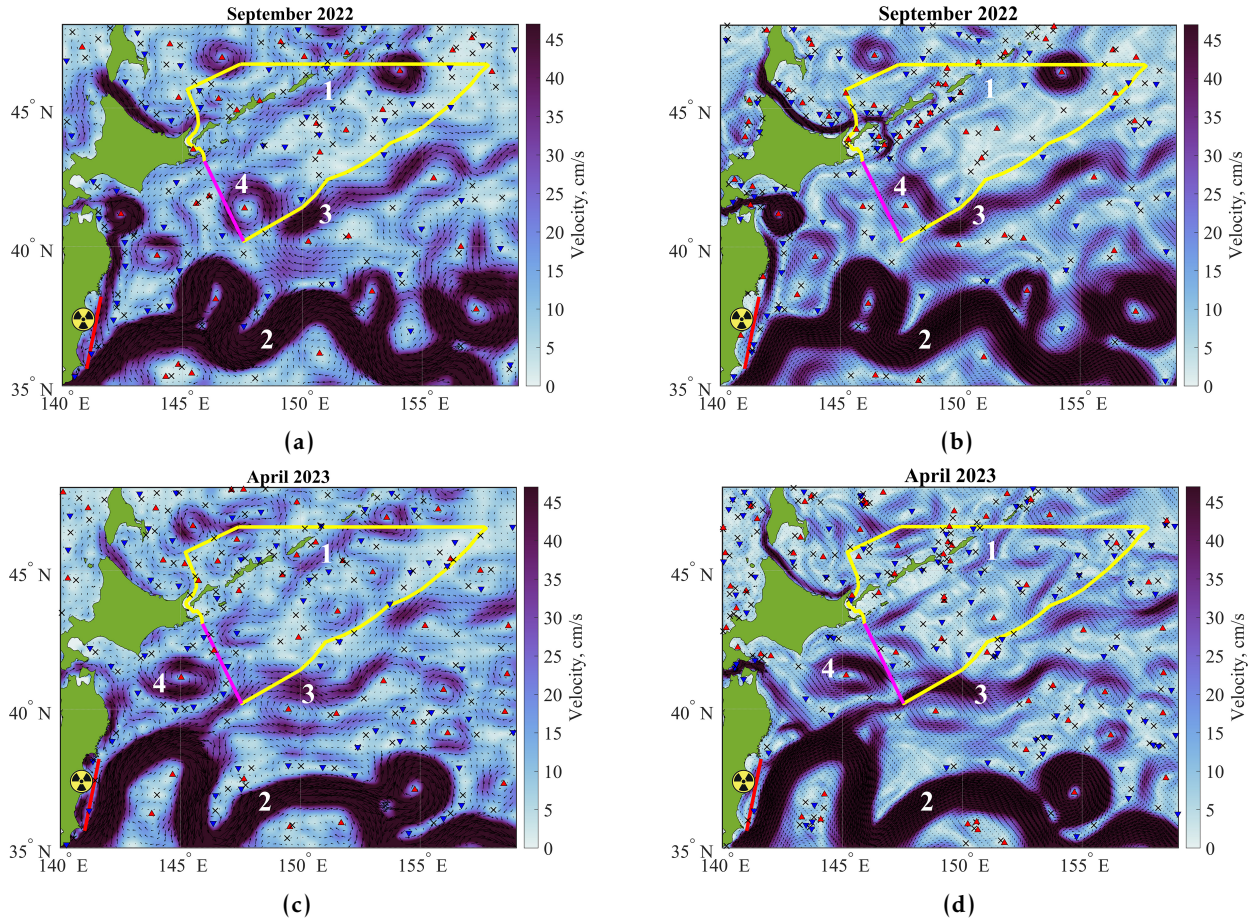

Figure 2. Geostrophic currents, derived from AVISO (left) and GLORYS12V1 (NEMO) (right) averaged for September 2022 and April 2023. Currents: 1 – Oyashio, 2 – Kuroshio, 3 – North Pacific Current, and 4 – quasistationary anticyclone. Arrows indicate current vectors, and the colour scale corresponds to the magnitude of the change in speed. The yellow line indicates the location of the SKFZ area; the pink line shows the boundary of the SKFZ closest to the Fukushima NPP. The red triangles ▲ correspond to anticyclone centres, and the blue triangles ▼ indicate cyclones. The black crosses represent the hyperbolic points.

To the east of Hokkaido in the region of 40°N, 150°E, there is a quasistationary anticyclone, and a cyclone is situated slightly to the north. Notably, in this part of the water body, north of the main Kuroshio current, there are several mesoscale eddies – cyclones and anticyclones – the centers of which are indicated in Figure 2 by blue and red triangles,

respectively. The generation of these eddies is mainly attributed to the meandering of the Kuroshio current and its barotropic and baroclinic instability [*Udalov et al.*, 2023]. This process is accompanied by the formation of an ordered system of anticyclones that propagate along the steep side of the Kuril Trench to the northeast, acquiring the characteristics of trench waves [*Gnevyshev et al.*, 2023; *Travkin et al.*, 2022]. Both cyclones and anticyclones, through rotation, while simultaneously moving northwards, can participate in the transport of potentially "contaminated" waters toward the shores of the Kuril Islands.

It is worth noting that calculations conducted with different datasets yield similar results so it is the validation of the model and of course it is related to the higher resolution of the model output, although it is fair to acknowledge that the number of eddies, as indicated by the blue and red triangles in Figure 2, differs between the AVISO and GLORYS12V1 (NEMO) data. This difference may be associated with the higher resolution of the velocity field in the GLORYS12V1 (NEMO) data.

4.2. Distribution of potentially "contaminated" waters in the study area

Every day from August 24, 2022, to August 24, 2023, a rectangular area with coordinates 40°–48.5°N, 145°–159°E was seeded with particles on a uniform grid of 700×700 nodes, totaling 49×10^4 markers. Then, for each particle, advection equations (1) were solved backward over 365 days, and trajectories were calculated. Figure 3 depicts the outcomes of Lagrangian modeling, illustrating the spatial distribution of Lagrangian particles and the recording of simulated particles in the study area. The experiment was conducted concurrently using AVISO and GLORYS12V1 (NEMO) data. The experiment unfolds as follows.

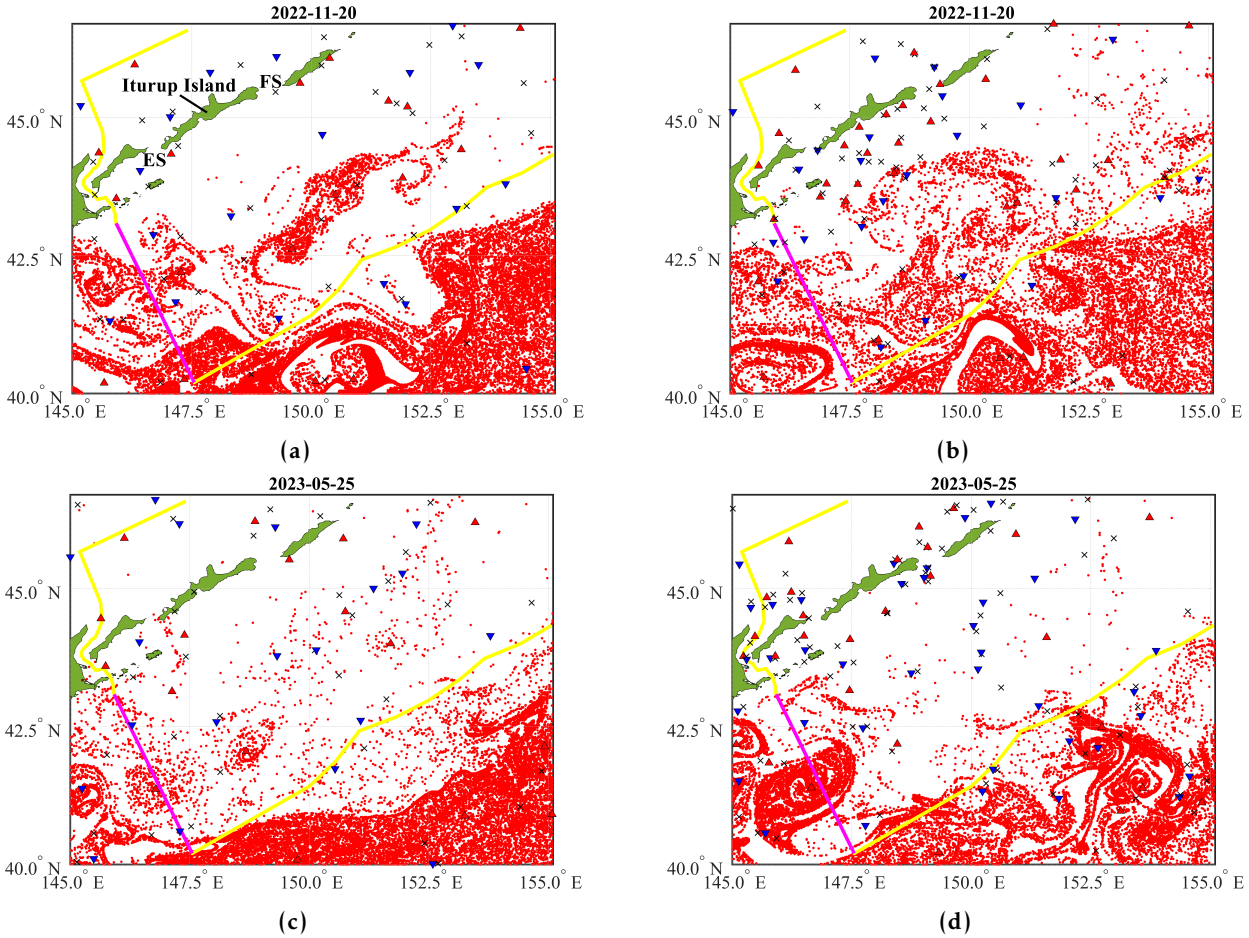

Figure 3. Spatial distribution of "contaminated" markers (shown as red dots) based on the altimetric AVISO (left) and GLORYS12V1 (NEMO) (right) data for specific dates: November 20, 2022, and May 25, 2023. Triangles and crosses represent the same features as in Figure 2. Green is the land; ES is the Ekaterina strait, and FS is the Friz strait.

The markers whose trajectories in the past intersected the segment 35.6°N, 141°E–38.2°N, 141.6°E (shown as a red line located close to the Fukushima NPP in Figure 1) were colored red and detected in Figure 3. These markers correspond to potentially simulated particles from the Fukushima NPP. Although, as claimed by many experts, the main portion of this water is indeed picked up by the Kuroshio Current and carried eastwards into the Pacific Ocean away from the shores of Japan, the potentially "contaminated" waters can be detected near the Kuril Islands. Figure 3 shows that the simulated particles reach the boundaries of the SKFZ and are carried northward. They also enter the Sea of Okhotsk through the Kuril Strait. Simulated particles emanating from the Fukushima NPP source outline circulation structures including eddies. Figure 3 shows that the primary concentration of the markers was outside the SKFZ. Indeed, the main portion of simulated particles from the Fukushima NPP, along with the Kuroshio, disperse eastwards. However, a substantial portion of them goes in a northern direction, crossing the boundaries of the SKFZ.

In Figure 3, we do not expect a 100% match in the distribution of markers, as the AVISO and GLORYS12V1 (NEMO) fields differ in spatial resolution and coastline shape. This causes markers in the AVISO field to "stick" near the shore, increasing their advection time in the study area. In the GLORYS12V1 field, a greater number of smaller-scale vortices are resolved, leading to the formation of compact "patches" of markers.

4.3. Temporal variability of simulated particle distribution from the Fukushima NPP

Then, we study temporal variability in the number of simulated particles the within the SKFZ based on AVISO and GLORYS12V1 (NEMO) data (Figure 4). All the markers that intersect the red segment in Figure 1 (the discharge boundary from the Fukushima NPP) are coloured red and are plotted of the map (see examples in Figure 3).

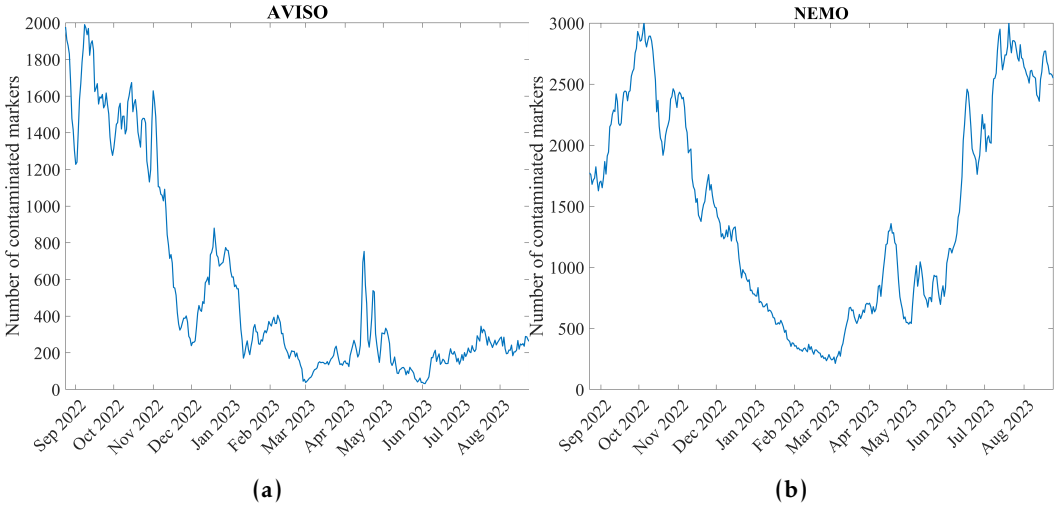

Figure 4. Temporal variability in the number of "contaminated" markers inside the SKFZ. The counts for AVISO and GLORYS12V1 (NEMO) data were collected daily from August 24, 2022, to August 24, 2023. The trajectory of each marker was calculated backward in time for a duration of 1 year.

Notably, the temporal variability plots calculated using the Lagrangian modeling but based on different datasets exhibited differences. The main distinction lies in the presence of peaks in the GLORYS12V1 (NEMO) data during the summer period, while these peaks are absent in the AVISO data.

This discrepancy may be attributed to the highly fragmented coastline in the AVISO data, which trapped some markers near the shore or this could be related to the different number of vortices in the GLORYS12V1 (NEMO) and AVISO data. The observed difference in the total number of simulated particles between the GLORYS12V1 (NEMO) and AVISO data may be attributed to the coastline resolution issue mentioned earlier. It is important to note, however, that both graphs show elevated values of simulated particles in September–

October, with a decrease during the winter period. Notably, the autumn season corresponds to the peak fishing period for most pelagic fish and squid in the SKFZ.

4.4. Estimation of the time required for simulated particles to reach the SKFZ boundary

Graphs illustrate the distribution of the number of simulated particles over time as they arrived at the southwest border of the SKFZ are shown in Figure 5. These graphs were generated using real-time marker advection data. Every day, from August 24, 2022, to June 6, 2023, 50,000 markers were launched on the red segment (Figure 1) near the eastern coast of Honshu. The choice of this segment is associated with the specific shape of the coastline according to AVISO data.

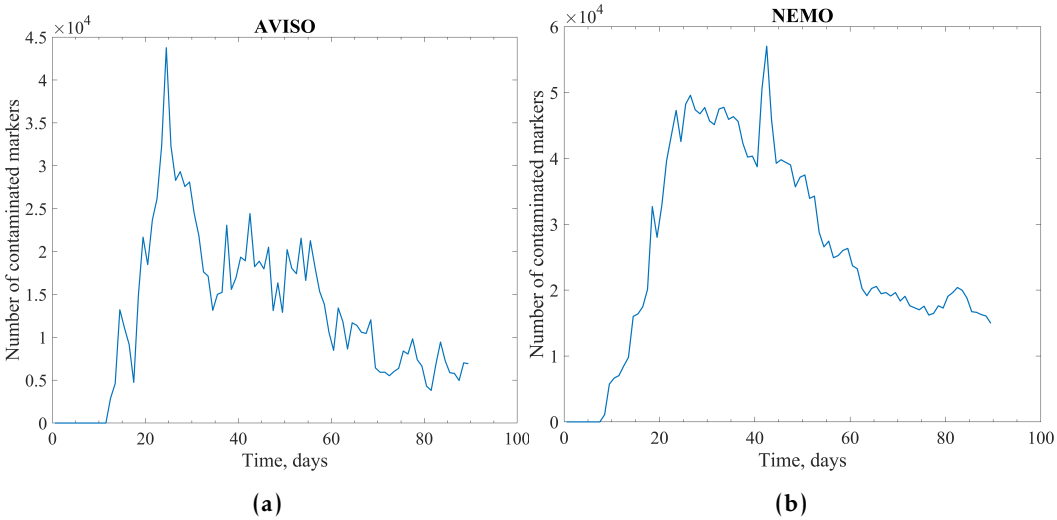

Figure 5. Distribution of the number of "contaminated" markers over time upon reaching the southern boundary of the SKFZ based on AVISO data (top) and GLORYS12V1 (NEMO) data (bottom). The abscissa axis represents days since the potentially "contaminated" waters discharge, and the ordinate axis represents the number of "contaminated" markers inside the SKFZ. Only markers that crossed the southern boundary of the SKFZ (pink segment in Figure 1) were considered.

Subsequently, each trajectory was calculated in real-time for 90 days after the launch date. In the graph calculated using the AVISO dataset, there is a prominent peak at 13 days. A similar peak is observed at 20 days in the GLORYS12V1 (NEMO) data, and the first simulated particles cross the SKFZ boundary just 8 days after the initial launch.

The first markers in GLORYS12V1 are advected to the selected segment somewhat faster than in AVISO because the coastline shape in AVISO is coarser, which may lead to delays in marker movement near the shore. The shift of the peak of "fast" markers towards higher travel times in GLORYS12V1 is related to the higher resolution of the velocity field in GLORYS12V1 compared to AVISO. This higher resolution in GLORYS12V1 reveals more vortex structures, which act as transport barriers to the unidirectional advection of markers from the release zone to the selected segment. Differences in the methodology of obtaining AVISO and GLORYS12V1 (NEMO) data, as well as in spatial resolution and temporal discretization, can lead to discrepancies in the results. It is important to note that both data sets indicate a potential hazard associated with the spread of contaminated waters. In this context, quantitative estimates are less significant than qualitative conclusions.

It is important to note that according to the GLORYS12V1 (NEMO) reanalysis data, simulated particles can reach SKFZ in just 8 days. The maximum values of simulated particles are 4.3×10^4 at 21 days according to AVISO data and 5.7×10^4 at 40 days according to GLORYS12V1 (NEMO) data. By 60 days after the discharge date, the number of simulated particles reaching SKFZ had decreased by 2–3 times but remained considerable.

4.5. Direct experiment involving the advection of the "contaminated" patch from the Fukushima NPP

The time required for the simulated particles to reach the boundaries of the South Kuril Fishing Zone (SKFZ) depends on the current circulation. This includes factors such as the shape and size of the Kuroshio meander (see Figure 2) and the local composition of mesoscale eddies with different polarities. Figure 6 identifies instances where the marker spot reached the boundaries of the SKFZ most rapidly. In the present study, the starting date was May 25, 2023.

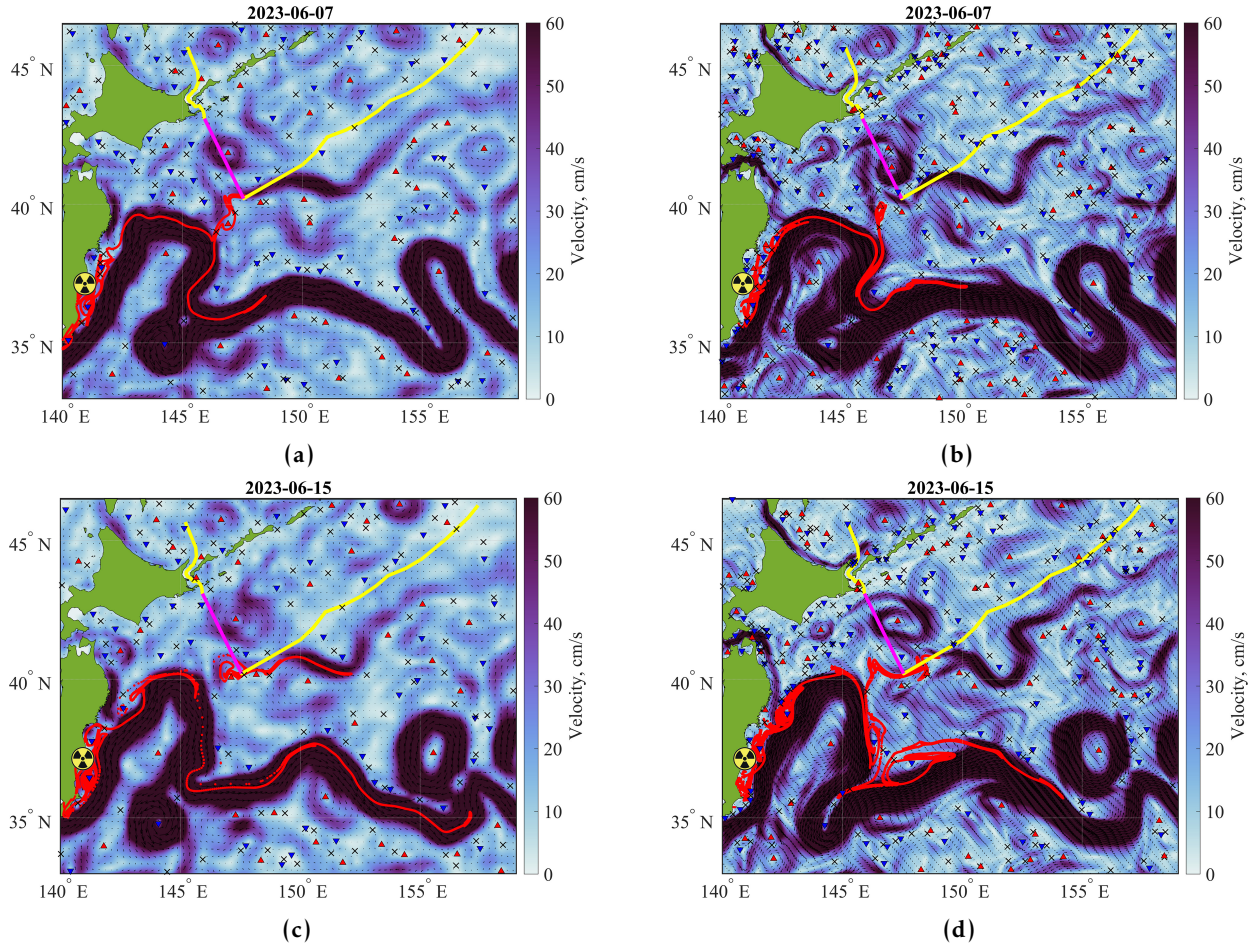

Figure 6. Velocity field based on AVISO data (left) and GLORYS12V1 (NEMO) data (right) showing the evolution of the patch of the "contaminated" markers from the Japanese coast near the Fukushima NPP (the segment, as well as the patch, are shown in red; see also Figure 1). The launch date of the markers is May 25, 2023. The "contaminated" markers reached the southwestern boundary of the SKFZ (indicated in pink) 13 days after launch.

It is important to note that the experiment tracking the fast advection of the patch from the Fukushima coast to the SKFZ was conducted similarly for both AVISO and GLORYS12V1 (NEMO). A total of 50,000 markers were released along the red segment (Figure 1) near the eastern coast of Honshu, after which the evolution of this patch was tracked. In Figure 6, images of the patch evolution 13 and 20 days after the launch date are shown. The rapid transport of markers is associated with the entrainment of the patch by the Kuroshio meander, which, during this period, was pressed against the eastern coast of Japan. The subsequent mechanism of advection of simulated particles into the SKFZ is linked to the detachment of a portion of the patch by the local system of mesoscale vortices that formed on the northern periphery of the Kuroshio meander. It is important to note that a similar mechanism of fast transport is observed in both the AVISO and GLORYS12V1 (NEMO) datasets.

Note the formation of characteristic U-shaped folds in the pollution patch as it passes near hyperbolic points (Figure 6) formed between the vortices and on the periphery of the Kuroshio meander. Such deformation leads to a rapid increase in the perimeter of the patch and additional expansion of the "polluted" area [*Prants et al.*, 2017c].

4.6. Dependence of the "contamination" in the South Kuril Fishing Zone on the date of potentially "contaminated" water discharge

The more important statement for this study is that as seen in previous analyses the particles following the north wall of the Kuroshio Extension eastward but tend to spread northward at the hyperbolic point mentioned. Figure 7 shows the distribution of the number of simulated particles reaching the South Kuril Fishing Zone (SKFZ) based on the date of their release. Importantly, we are examining a hypothetical scenario in which simulated particles are released from August 24, 2022, to August 24, 2023. Each day, 50,000 markers were released along the red segment (see Figure 1). The obtained estimates vary between the different datasets of AVISO and GLORYS12V1 (NEMO).

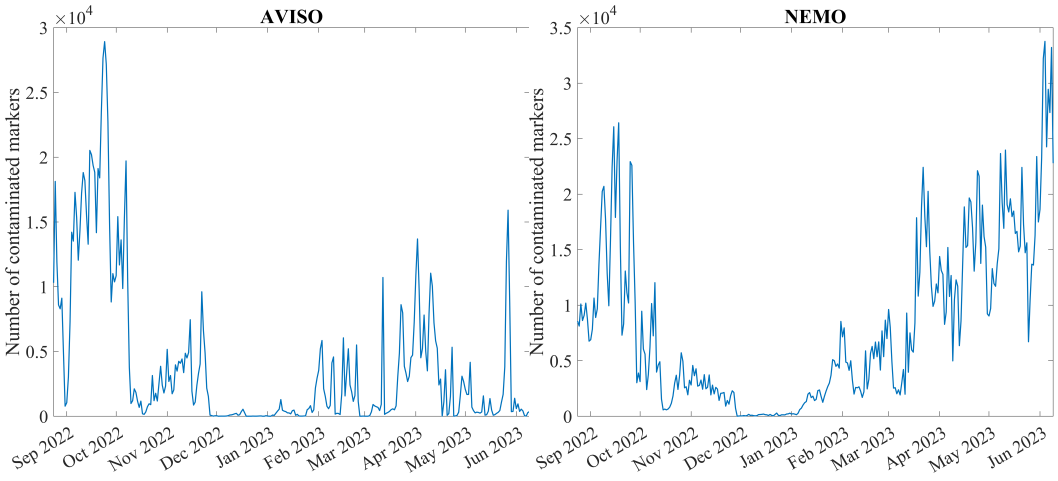

Figure 7. Distribution of the number of "contaminated" markers reaching the southwest border of the SKFZ based on the dates of their release from the Japanese coast (red segment in Figure 1). The AVISO data (top) and GLORYS12V1 (NEMO) data (bottom) are used.

If discharge occurs in December-January, only a negligible number of simulated particles enter the South Kuril fishing zone (SKFZ). The opposite situation is observed in other months when the number of markers is measured in tens of thousands. It is noteworthy that the obtained estimates vary for different datasets: a maximum of 2.75×10^4 is reached in October 2022 according to AVISO data, and 3.75×10^4 is reached in June 2023 according to GLORYS12V1 (NEMO) data. This implies that the discharge of simulated particles in these months leads to significant contamination of the SKFZ, and the period from December to January is the most favourable period for discharge.

It is important to note that we analysed only a single year of data so the results are presented as an example of the variability one might expect.

4.7. Density of tracer tracks of the potentially "contaminated" markers

In Figure 8, sets of maps depicting the density of trajectories of tracers (dasymetric maps) are presented for simulated particles launched near the eastern coast of Japan during September, November 2022, and April 2023. To construct these maps, we divide the study area (35–44°N, 140°–150°E) into a uniform grid of 400×400 rectangular cells. For each cell, the daily count of tracks left by the trajectories of simulated particles was then calculated.

The mechanisms of their transport to the boundary of the SKFZ and, consequently, the estimates of density and spatial distribution of traces depend on the existing hydrological regime in the region. In some periods, the regime is influenced primarily by the developing

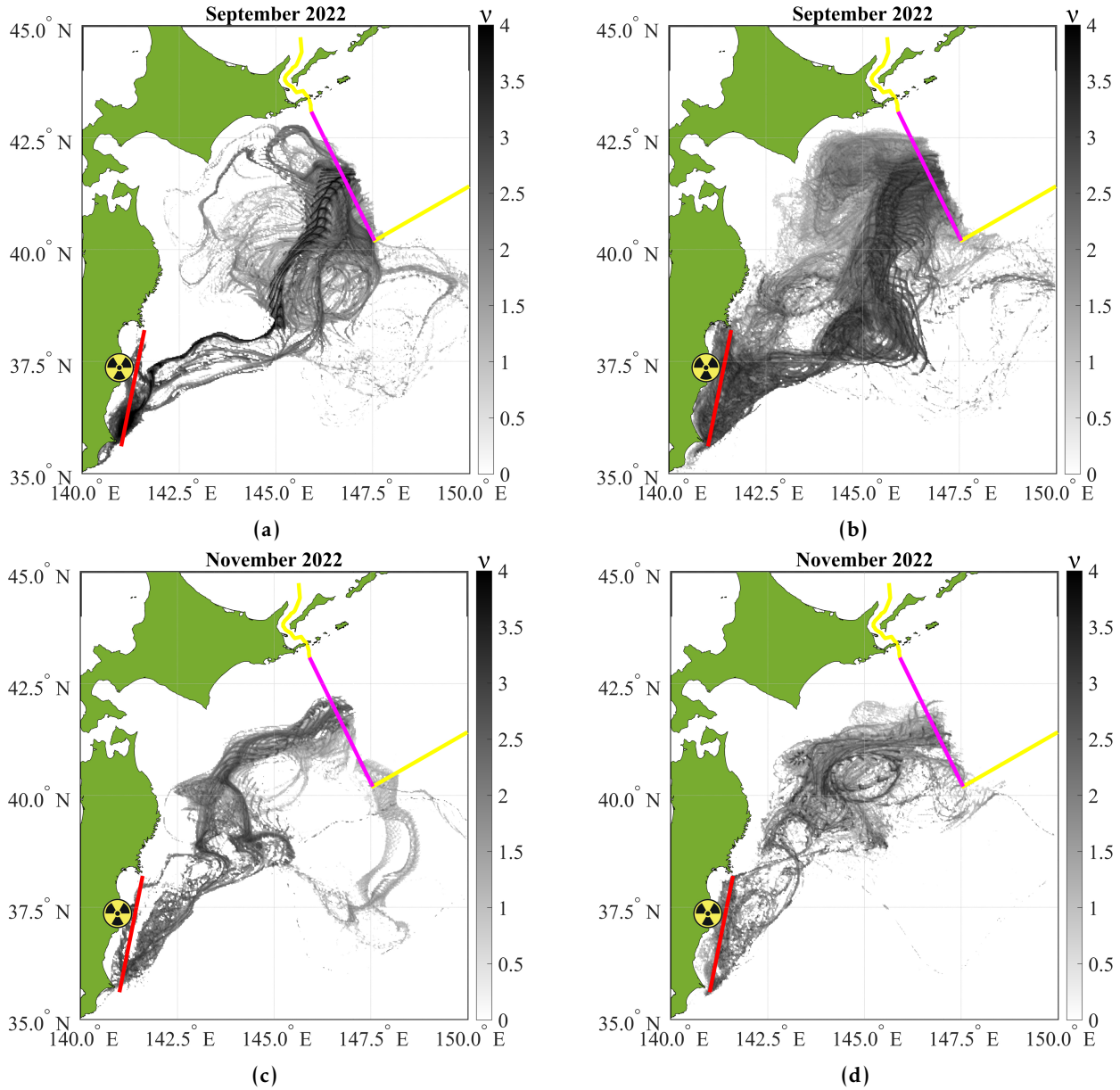

Figure 8. Density (dasymetric) maps of "contaminated" markers trajectories released from the Fukushima NPP in September, November 2022, and April 2023, reaching the southwest segment of the SKFZ. The calculation is based on AVISO data (left) and GLORYS12V1 (NEMO) data (right). The scale presents $\nu = log\varphi$, where φ is the density of daily tracks of the trajectories.

first meander of the Kuroshio Current, while in others, mesoscale vortex advection takes precedence.

It is important to note that the shapes of the patches for the same months are very similar on the maps calculated based on the AVISO velocity field and the GLORYS12V1 (NEMO) reanalysis. However, according to the modeling results based on GLORYS12V1 (NEMO), the density of the traces is greater than that from the AVISO data. This difference could be attributed to a greater number of markers trapped near the coast when computing trajectories based on AVISO data. The coastline mask of Honshu Island is more jagged in AVISO than in GLORYS12V1 (NEMO).

4.8. Distribution of the number of simulated particles by the date of arrival at the boundary of the SKFZ

The distribution of the markers by the date that they reached the southwest boundary of the SKFZ is shown in Figure 9. The presence of peaks in certain months indicates that

more careful dosimetry should be conducted during these months when organizing fishing activities.

According to AVISO, the highest penetration of simulated particles occurs in November 2022, when the penetration reaches 15×10^4 however, in other months, this number does not exceed 3×10^4. According to the GLORYS12V1 (NEMO) data, several peaks of $3–5 \times 10^4$ were identified for different months, with the maximum values also occurring in November 2022. This indicates that the highest number of simulated particles reached the boundary of the SKFZ in November. The lowest number of markers reached the SKFZ boundary during the period from February to April.

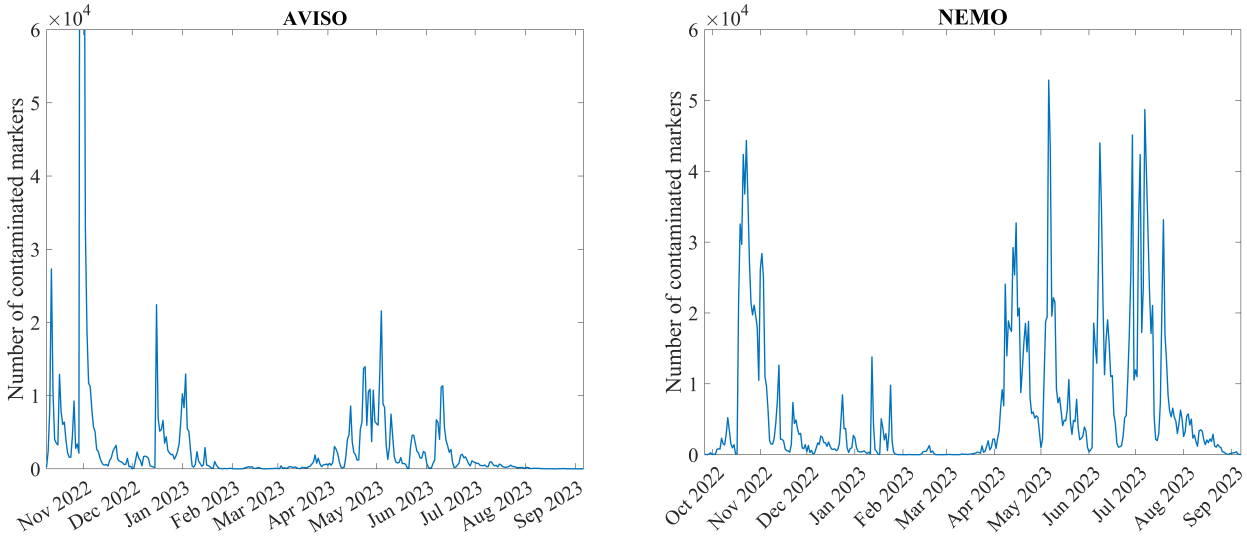

Figure 9. Distribution of the number of "contaminated" markers by the date of arrival at the southwest border of the SKFZ since August 24, 2022.

5. Discussion and Conclusions

A series of studies analysing the spread of radioactive contamination in the ocean emerged [see reviews in works by *Budyansky et al.*, 2015; *Prants*, 2014; *Prants et al.*, 2017a,b,c] These studies utilized in situ measurements of radionuclide concentrations and altimetric velocity fields constructed from satellite measurements. Lagrangian modeling methods were employed to simulate the dispersion of potentially simulated particles. Research has shown that the primary mechanisms contributing to the spread of contamination in the Pacific Ocean include existing ocean current systems and vortex advection.

Using the Lagrangian approach, we focus on the advection of simulated particles from the Fukushima NPP called here simulated particles and solve the problems of identifying their transport corridors. We also study the seasonal variability of this advection. A similar approach was previously used by the authors in modeling the transfer of caesium 137 and 134 after the Fukushima NPP accident in the period from 2011 to 2021 based on the AVISO velocity field [*Budyansky et al.*, 2015, 2022].

Thus, the purpose of this work is to identify the possible transport corridors and mechanisms of advection from sites where potentially "contaminated" waters are discharged from the Fukushima NPP. This study is based on two types of data: 1) current velocity fields calculated from satellite altimetry data provided by AVISO and 2) velocities extracted from the global high-resolution reanalysis, GLORYS12V1 (NEMO). The calculation of the advection of markers in the GLORYS12V1 (NEMO) field for this area is new. We employ some original approaches like dasymetric maps developed within the framework of Lagrangian modeling to study the advection of potentially "contaminated" waters in areas that are

adjacent to the Kuril Ridge. Note, that this is a region of traditional Russian fisheries for fish and squid.

The chosen analysis period spans one year before the actual discharge of potentially "contaminated" waters, i.e., from August 24, 2022, to August 24, 2023. Note that a comparison of the charts for AVISO and GLORYS12V1 (NEMO) reveals a good correspondence in terms of the times and paths of arrival, and most importantly, that the transfer mechanisms coincide i.e. picking up by the Kuroshio meander and advection by a local vortex system.

The main conclusion drawn from this study is that the potentially "contaminated" waters can arrive in the areas of commercial fisheries for fish and squid in the SKFZ. The primary mechanisms through which these simulated particles reach fishing areas are the meandering of the Kuroshio current and vortex advection. During the spring months, the first Kuroshio meander closely approaches the coasts of Japan, while the existing system of cyclones and anticyclones to the north carries simulated particles into the fishing areas. These markers gradually accumulate and disperse across the region.

We found that there is a regime in which simulated particles from the Fukushima NPP can cross the southwestern boundary of the subarctic frontal zone (SKFZ) within 8–13 days. This situation corresponds to the time when the first meander of the Kuroshio Current approaches the eastern coast of Hokkaido. We conducted a direct experiment on the transport of marker patches from the release of Fukushima NPP water and analysed their trajectories. The marker patch elongates into a strip along the northern flank of the meandering Kuroshio current. However, some markers break away from the initial patch and are then picked up by the system of mesoscale vortices, which push these markers into the SKFZ.

This study demonstrates one of the possible mechanisms for the entry of simulated particles into the SKFZ. We analysed the dependence of the number of simulated particles in the SKFZ on the date of potentially "contaminated" waters release. It is revealed that the most unfavourable months for release for the SKFZ are the summer and autumn months. A strong seasonal dependence of the advection of a large number of simulated particles into the fishing zone is demonstrated, depending on the discharge month. Thus, during the period from 2022 to 2023, when discharged in certain months, the quantity of markers exceeds several times the amount discharged in winter – a difference of several orders of magnitude specifically for the considered year. Conversely, the lowest risk of potential "contamination" is observed in December and January. The more important statement for this study is that as seen in previous analyses the particles following the north wall of the Kuroshio Extension eastward but tend to spread northward at the hyperbolic point mentioned.

The dasymetric maps we constructed depict the so-called "transport corridors" through which potentially "contaminated" waters enter the SKFZ. In different months, these "transport corridors" have varying widths and densities, depending on the quantity of simulated particles.

We also analysed the number of simulated particles in the SKFZ based on the dates of their arrival at the southwestern border of the Kuril-Kamchatka Trench. The highest number of simulated particles reached the border in November 2022. This implies that more careful dosimetry should be conducted in November during the organization of fishing activities in the SKFZ.

Although recent releases from Fukushima NPP are projected to have minimal impacts on seafood consumers and the marine ecosystem, as indicated by various studies and reports [*IAEA*, 2018, 2023; *Maderich et al.*, 2024; *Smith et al.*, 2023; *TEPCO*, 2023, and references herein], our research underscores the critical importance of continuous monitoring in the region including the SKFZ. This imperative arises from several key factors that warrant sustained attention and surveillance. Firstly, the dynamic nature of ocean currents can disperse contaminants over vast distances so it necessitates ongoing monitoring to track the trajectory and dispersion patterns of released substances. Secondly, the complexity of interactions within marine ecosystems requires constant vigilance to detect any subtle

changes or unexpected consequences that may arise from the Fukushima NPP releases. This includes monitoring the health and behaviour of marine organisms, as well as assessing any alterations in biodiversity and ecosystem dynamics. Furthermore, the evolving nature of environmental conditions, influenced by factors such as climate change and other anthropogenic stressors, underscores the need for continuous monitoring to adapt and refine our understanding of the potential impacts of Fukushima NPP releases in a changing environment.

AVISO and GLORYS12V1 (NEMO) are two distinct sources of information that are not required to duplicate each other. AVISO provides data based on satellite measurements, whereas the GLORYS12V1 reanalysis utilizes the NEMO hydrodynamic model, which is based on the equations of motion. Differences in the methodology of obtaining data from AVISO and GLORYS12V1 (NEMO), as well as in spatial resolution and temporal discreteness, can lead to discrepancies in the results. It is important to note that both data sets indicate a potential hazard related to the spread of "contaminated" waters. In this context, qualitative conclusions are more significant than quantitative assessments. The main conclusion is that regardless of the type of data chosen, the potential hazard of spreading "contaminated" waters must be taken into account.

It is apparent that Japan has chosen the most cost-efficient way to deal with the contaminated water; however, great opposition and concerns have been aroused internationally due to the harmful ecotoxicological features of radioactive materials [*Bezhenar et al.*, 2021; *Lu et al.*, 2021]. Moreover, several scientists believe that it is necessary to organize not only dosimetric but also spectrometric monitoring during fishing activities in months with higher contamination levels in the Kuril zone [*Paraskiv et al.*, 2022]. Unlike many studies that analyze the concentrations of radioactive isotopes and their toxicological harm to biota using various methods [*Bezhenar et al.*, 2021; *Lu et al.*, 2021; *Men*, 2021], our research focuses on studying the pathways of potentially contaminated water and the time it takes for these waters to reach the area of traditional Russian fishing. We demonstrate the possibility of their entry into the coastal waters of the Kuril region and show that there is a possibility of minimizing damage, which is determined by choosing the optimal dates for discharging contaminated technical waters from the Fukushima NPP.

In conclusion, although preliminary evaluations may imply negligible immediate risks, the complex and interrelated dynamics within marine systems necessitate continuous monitoring to ensure a thorough comprehension of the persistent implications arising from the discharge of water from Fukushima NPP. This sustained vigilance is imperative for the preservation of marine ecosystems and the cultivation of trust among seafood consumers in the respective region. Enhancing the understanding of marker advection processes will serve to optimize the ongoing monitoring efforts.

Acknowledgements. The research was carried out with the support of St. Petersburg University, grant No. 116442164. The work of M.B. and A.U. on the Lagrangian analysis of passive marker advection is supported by the Russian Science Foundation (RSF) (grant No. 23-17-00068) with the help of a high-performance computing cluster at the Pacific Oceanological Institute (State Task No. 124022100072-5).

References

Belonenko, T. V., D. K. Staritsyn, V. R. Foux, et al. (1997), *The Origins of Oyasio*, 248 pp., St. Petersburg State University, St. Petersburg (in Russian).

Belonenko, T. V., V. V. Koldunov, D. K. Staritzyn, et al. (2009), *Sea-sureface level variability in the North-western Pacific*, 309 pp., SMIO Press, Saint-Petersburg (in Russian).

Bezhenar, R., H. Takata, G. de With, and V. Maderich (2021), Planned release of contaminated water from the Fukushima storage tanks into the ocean: Simulation scenarios of radiological impact for aquatic biota and human from seafood consumption, *Marine Pollution Bulletin*, *173*, 112,969, https://doi.org/10.1016/j.marpolbul.2021.112969.

Budyansky, M. V., V. A. Goryachev, D. D. Kaplunenko, et al. (2015), Role of mesoscale eddies in transport of Fukushima-derived cesium isotopes in the ocean, *Deep Sea Research Part I: Oceanographic Research Papers*, *96*, 15–27, https://doi.org/10.1016/j.dsr.2014.09.007.

Budyansky, M. V., P. A. Fayman, M. Y. Uleysky, and S. V. Prants (2022), The impact of circulation features on the dispersion of radionuclides after the nuclear submarine accident in Chazhma Bay (Japan Sea) in 1985: A retrospective Lagrangian simulation, *Marine Pollution Bulletin*, *177*, 113,483, https://doi.org/10.1016/j.marpolbul.2022.113483.

Buslov, A. V. (Ed.) (2013), *Fishing Resources Harvesting in the Waters of the Kuril Ridge: Modern Structure, Dynamics and Key Elements*, 264 pp., SakhNIRO, Yuzhno-Sakhalinsk (in Russian).

CMEMS (2020), *Product user manual for sea level SLA products. CMEMS-SL-PUM-008-032-062.*

Dong, D., P. Brandt, P. Chang, et al. (2017), Mesoscale Eddies in the Northwestern Pacific Ocean: Three-Dimensional Eddy Structures and Heat/Salt Transports, *Journal of Geophysical Research: Oceans*, *122*(12), 9795–9813, https://doi.org/10.1002/2017JC013303.

Gnevyshev, V. G., V. S. Travkin, and T. V. Belonenko (2023), Topographic Factor and Limit Transitions in the Equations for Subinertial Waves, *Fundamental and Applied Hydrophysics*, *16*(1), 8–23, https://doi.org/10.48612/fpg/92rg-6t7h-m4a2.

IAEA (2018), Regulatory control of radioactive discharges to the environment, *Tech. rep.*, International Atomic Energy Agency.

IAEA (2023), IAEA Comprehensive Report on the Safety Review of the ALPS-Treated Water at the Fukushima Nuclear Power Station, *Tech. rep.*, International Atomic Energy Agency.

Itoh, S., and I. Yasuda (2010), Water Mass Structure of Warm and Cold Anticyclonic Eddies in the Western Boundary Region of the Subarctic North Pacific, *Journal of Physical Oceanography*, *40*(12), 2624–2642, https://doi.org/10.1175/2010JPO4475.1.

Kawai, H. (2013), Hydrography of the Kuroshio Extension, in *Kuroshio: Physical Aspects of the Japan Current*, pp. 235–352, University of Washington Press.

Kawakami, Y., S. Sugimoto, and T. Suga (2015), Inter-annual zonal shift of the formation region of the lighter variety of the North Pacific Central Mode Water, *Journal of Oceanography*, *72*(2), 225–234, https://doi.org/10.1007/s10872-015-0325-1.

Lellouche, J.-M., E. Greiner, R. Bourdallé-Badie, et al. (2021), The Copernicus Global 1/12° Oceanic and Sea Ice GLORYS12 Reanalysis, *Frontiers in Earth Science*, *9*, https://doi.org/10.3389/feart.2021.698876.

Lu, Y., J. Yuan, D. Du, B. Sun, and X. Yi (2021), Monitoring long-term ecological impacts from release of Fukushima radiation water into ocean, *Geography and Sustainability*, *2*(2), 95–98, https://doi.org/10.1016/j.geosus.2021.04.002.

Maderich, V., D. Tsumune, R. Bezhenar, and G. de With (2024), A critical review and update of modelling of treated water discharging from Fukushima Daiichi NPP, *Marine Pollution Bulletin*, *198*, 115,901, https://doi.org/10.1016/j.marpolbul.2023.115901.

Men, W. (2021), Discharge of contaminated water from the Fukushima Daiichi Nuclear Power Plant Accident into the Northwest Pacific: What is known and what needs to be known, *Marine Pollution Bulletin*, *173*, 112,984, https://doi.org/10.1016/j.marpolbul.2021.112984.

NOAA (2013), Severe Marine Debris Event Report: Japan Tsunami Marine Debris. Overview and Update to Congress, *Tech. rep.*, U.S. Department of Commerce.

Oka, E., and B. Qiu (2011), Progress of North Pacific mode water research in the past decade, *Journal of Oceanography*, *68*(1), 5–20, https://doi.org/10.1007/s10872-011-0032-5.

Oka, E., S. Kouketsu, K. Toyama, et al. (2011), Formation and Subduction of Central Mode Water Based on Profiling Float Data, 2003-08, *Journal of Physical Oceanography*, *41*(1), 113–129, https://doi.org/10.1175/2010JPO4419.1.

Paraskiv, A. A., N. N. Tereshchenko, V. Y. Proskurnin, et al. (2022), Accumulation Ability of Hydrobionts and Suspended Matter in Relation to Plutonium Radioisotopes in Coastal Waters (Sevastopol Bay, the Black Sea), *Vestnik Tomskogo gosudarstvennogo universiteta. Biologiya*, (60), 78–101, https://doi.org/10.17223/19988591/60/5.

Prants, S. V. (2014), Chaotic Lagrangian transport and mixing in the ocean, *The European Physical Journal Special Topics*, *223*(13), 2723–2743, https://doi.org/10.1140/epjst/e2014-02288-5.

Prants, S. V., M. V. Budyansky, and M. Y. Uleysky (2017a), Lagrangian simulation and tracking of the mesoscale eddies contaminated by Fukushima-derived radionuclides, *Ocean Science*, *13*(3), 453–463, https://doi.org/10.5194/os-13-453-2017.

Prants, S. V., M. V. Budyansky, and M. Y. Uleysky (2017b), Statistical analysis of Lagrangian transport of subtropical waters in the Japan Sea based on AVISO altimetry data, *Nonlinear Processes in Geophysics*, *24*(1), 89–99, https://doi.org/10.5194/npg-24-89-2017.

Prants, S. V., M. Y. Uleysky, and M. V. Budyansky (2017c), *Lagrangian Oceanography: Large-scale Transport and Mixing in the Ocean*, Springer International Publishing, https://doi.org/10.1007/978-3-319-53022-2.

Qiu, B., P. Hacker, S. Chen, et al. (2006), Observations of the Subtropical Mode Water Evolution from the Kuroshio Extension System Study, *Journal of Physical Oceanography*, *36*(3), 457–473, https://doi.org/10.1175/JPO2849.1.

Qu, T., H. Mitsudera, and B. Qiu (2001), A Climatological View of the Kuroshio/Oyashio System East of Japan, *Journal of Physical Oceanography*, *31*(9), 2575–2589, https://doi.org/10.1175/1520-0485(2001)031<2575:ACVOTK>2.0.CO;2.

Sekine, Y., and K. Kutsuwada (1994), Seasonal Variation in Volume Transport of the Kuroshio South of Japan, *Journal of Physical Oceanography*, *24*(2), 261–272, https://doi.org/10.1175/1520-0485(1994)024<0261:SVIVTO>2.0.CO;2.

Shuntov, V. P. (2022), *Biology of the Far Eastern Seas of Russia*, *Volume 3*, 445 pp., TINRO Center, Vladivostok (in Russian).

Smith, J., N. Marks, and T. Irwin (2023), The risks of radioactive wastewater release, *Science*, *382*(6666), 31–33, https://doi.org/10.1126/science.adi5446.

Suga, T., and K. Hanawa (1995), The Subtropical Mode Water Circulation in the North Pacific, *Journal of Physical Oceanography*, *25*(5), 958–970, https://doi.org/10.1175/1520-0485(1995)025<0958:TSMWCI>2.0.CO;2.

TEPCO (2023), Partial Revision of the Application for approval to amend the Implementation Plan for Fukushima Daiichi Nuclear Power Station as Specified Nuclear Facility, *Tech. rep.*, Tokyo Electric Power Company Holdings.

Tomosada, A. (1986), Generation and decay of Kuroshio warm-core rings, *Deep Sea Research Part A. Oceanographic Research Papers*, *33*(11–12), 1475–1486, https://doi.org/10.1016/0198-0149(86)90063-4.

Travkin, V. S., T. V. Belonenko, and A. V. Kochnev (2022), Topographic waves in the Kuril region, *Sovremennye problemy distantsionnogo zondirovaniya Zemli iz kosmosa*, *19*(5), 222–234, https://doi.org/10.21046/2070-7401-2022-19-5-222-234 (in Russian).

Udalov, A., M. Budyansky, and S. Prants (2023), A census and properties of mesoscale Kuril eddies in the altimetry era, *Deep Sea Research Part I: Oceanographic Research Papers*, *200*, 104,129, https://doi.org/10.1016/j.dsr.2023.104129.

Venti, N. L., and K. Billups (2013), Surface water hydrography of the Kuroshio Extension during the Pliocene-Pleistocene climate transition, *Marine Micropaleontology*, *101*, 106–114, https://doi.org/10.1016/j.marmicro.2013.02.004.

Zhang, Z., H. Nakamura, and X.-H. Zhu (2021), Seasonal velocity variations over the entire Kuroshio path part II: dynamical interpretation for the current speed variation, *Journal of Oceanography*, *77*(5), 745–761, https://doi.org/10.1007/s10872-021-00603-8.